JOURNAL OF MATERIALS SCIENCE: MATERIALS IN MEDICINE 3 (1992) 106–113

Small diameter polyurethane–polydimethylsiloxane vascular prostheses made by a spraying, phase-inversion process

G. SOLDANI
Istituto di Fisiologia Clinica del CNR, Via Diotisalvi, 2-56100 Pisa, Italy
G. PANOL, H. F. SASKEN, M. B. GODDARD, P. M. GALLETTI
Artificial Organ Laboratory, Brown University, Providence, RI 02912, USA

A highly porous, distensible, gel-like tubular membrane suitable for a small diameter arterial prosthesis was fabricated by combining techniques for spraying and phase-inversion of thermodynamically unstable solutions of a biocompatible polyurethane (PU)–polydimethylsiloxane (PDMS) blend (Cardiothane $^{TH}51$) over a sliding and rotating mandrel. The cylindrical membrane was characterized *in vitro* for mechanical, morphological and permeability properties, and evaluated *in vivo* as a 1.5 mm internal diameter prosthesis for the replacement of the rat abdominal aorta. A mature, stable luminal interface, a thin internal capsule without anastomotic hyperplasia, and the deposition of collagen within the voids of the polymer mesh were observed after 8 weeks of implantation.

1. Introduction

Vascular prostheses made of porous fabrics such as expanded polytetrafluoroethylene (Teflon®) and woven or knitted polyethyleneterephthalate (Dacron®), although successful in the replacement of large diameter arteries, have not proven useful for long term applications as venous or small diameter arterial substitutes [1, 2]. Therefore, new approaches to the fabrication of small diameter vascular prostheses are still warranted. The challenge is to design a tubular structure 1 to 4 mm internal diameter (i.d.) which can remain patent in a low blood flow configuration, does not induce anastomotic hyperplasia, and promotes a minimal connective tissue growth on the luminal surface to support the formation of a thin, stable, mature neointima. Chemical composition [3–5], method of fabrication [6], compliance [7–10], porosity [11], and bioresorbability [12, 13] all appear to influence neointima formation, however, wall porosity seems to play a critical role in the healing process and is therefore a key factor for the long term success of synthetic small diameter vascular prostheses [14–16].

Numerous techniques have been described to produce porous or filamentous small diameter tubular fabrics from polyurethanes. For example, White and co-workers [17, 18] developed a replamineform template process using calcite derived from sea urchin spines. The spines were machined into tubes of the desired diameter and wall thickness and then pressure injected with a polyurethane solution. Following solvent evaporation, the calcite was dissolved with hydrochloric acid, leaving a polymer wall structure with interconnected pores. The Lyman *et al.* [19] technique for producing porous, compliant prostheses consisted of repeated cycles of dipping a glass mandrel in a copolyetherurethane–urea using N, N–dimethylformamide (DMF) as a solvent, and precipitation in water. Annis *et al.* [20] prepared filamentous polyurethane tubes by electrostatic spinning, a process in which a highly porous and distensible non-woven fabric was formed by ejecting a polymer solution from a syringe on to a sliding, rotating steel mandrel through an electrostatic field obtained by maintaining the mandrel at − 20 kV. Leidner *et al.* [21], extruded a polymer in the liquid phase (either melted or dissolved in a solvent) through fine orifices to form fibres which could be stretched and wound on to a rotating mandrel. Recently, Kowligi *et al.* [22], described a spraying technique to apply a fine mixture of polymer solution and nitrogen gas bubbles on to a rotating mandrel.

Our own approach to vascular prostheses fabrication combines aspects of several of the processes described above, but relies on a thermodynamically unstable polymer solution which can readily form a gel upon exposure to a relatively small excess of a nonsolvent, producing a material which displays a fine interconnected pore structure. This process involves the formation of gel-like tubular membranes by a phase-inversion effect derived from simultaneous but separate spraying of a PU–PDMS solution and water (as nonsolvent) over a sliding and rotating mandrel. This report describes the fabrication process, the physical characterization of the membrane structure, and the healing response of tubular membrane segments implanted as rat abdominal aorta substitutes.

0957–4530

2. Materials and Methods

2.1. Membranes fabrication process

Cardiothane TH51 (Kontron Instruments Inc., Everett, MA), a blend of PU (90%) and PDMS (10%) which also contains the copolymer of both components [23], was used because of: (1) Its excellent solubility and stability in relatively low boiling point, water miscible solvents such as tetrahydrofuran (THF) and 1,4 dioxane; (2) its excellent elastomeric properties and (3) its relatively good blood compatibility, as already shown with artificial hearts, intra-aortic balloons, catheters, and blood conduits [24].

The commercially available 16% w/v solution of Cardiothane TH51 in 2:1 THF/1,4 dioxane was diluted with a distilled 2:1 THF/1,4 dioxane solvent mixture (Kontron Instruments Inc., Everett, MA) to reach a polymer concentration of 1% w/v. Immediately before use, we added 16.5 ml of distilled water to each 100 ml of dilute polymer solution to achieve a clear 0.86% w/v polymer–solvent–nonsolvent system which would precipitate with the addition of a small amount of water. To obtain highly porous membranes, the polymer solution must be subjected to a process referred to by Kesting as phase-inversion [25]. This process has also been used by Wijmans [26] to study phase separation phenomena in ternary solutions of polysulphone in solvent–nonsolvent mixtures. The nonsolvent tolerance of our polymer solution was estimated by placing 100 ml of it in a vessel maintained at a temperature of 25 °C under gentle stirring, and then, using a titration burette, slowly adding to the solution, distilled water as a nonsolvent until incompatibility was visually detected by the appearance of turbidity or actual precipitation.

To fabricate the membranes, we designed and built a small precision lathe in which mandrels of different diameters could be rotated at speeds from 0 to 5000 r.p.m. using an electronically controlled variable speed motor. Parallel to the axis of the lathe we positioned a carriage which could move bidirectionally along the axis of the rotating mandrel (Fig. 1) powered by a motor which could be automatically reversed by the action of electromechanical relays controlled by micro-switches. Two modified spray guns were mounted horizontally on the carriage and positioned so the centreline of the nozzles and the mandrel lay in the same plane. The distance and angle between the mandrel and the nozzles was adjusted so

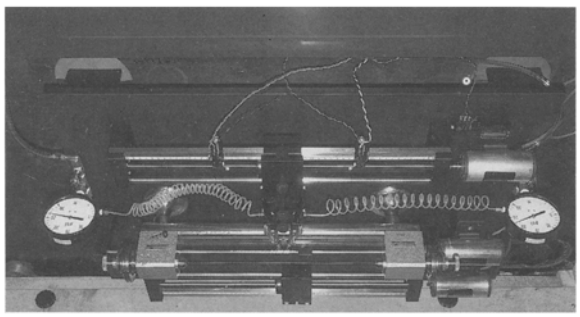

Figure 1 Apparatus for the fabrication of gel-like tubular membranes.

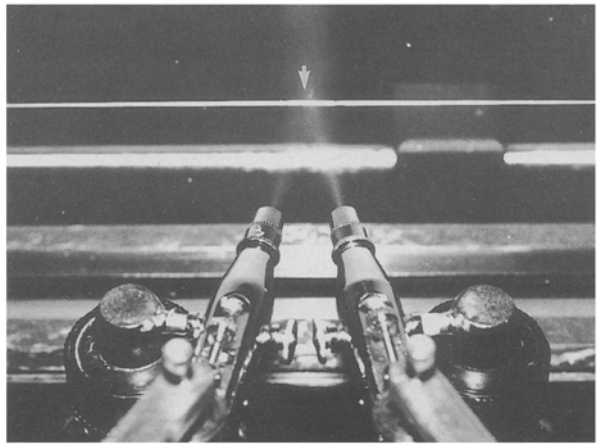

Figure 2 Detail of Fig. 1, showing the spray guns in angled position with their jet streams converging over the mandrel (arrow).

that the intersection of the jets occurred at the surface of the mandrel (Fig. 2). The mixing chamber of each spray gun was equipped with two ports, one connected by a short stainless steel adapter to a 100 ml glass reservoir for the polymer solution or the precipitating fluid, the other connected by Teflon tubing to a compressed nitrogen tank equipped with a flow regulator and a pressure gauge.

To fabricate a membrane, the two glass reservoirs were filled, one with the polymer solution and the other with distilled water, and the two fluids were simultaneously but separately sprayed at the same flow rate on to a Teflon (Small Parts Inc., Miami, FL) rotating mandrel, previously cleaned with a 0.5% solution of Triton X-100 (SIGMA, St. Louis, MO) in water. The mandrel rotation speed and carriage movement speed were set at predetermined values, and both water and the polymer solution were sprayed at predetermined pressure, angles, and distances between nozzles and mandrel. The entire process was carried out in a chemical fume hood. Wall thickness was closely related to the volume of polymer solution sprayed. When a desired end point was reached, the process was stopped and the Teflon mandrel with the deposited material was submerged overnight in a bath of deionized water in order to cure the delicate sponge-like structure of the membrane by allowing exchange of the solvent system for the nonsolvent. The finished membrane was removed from the mandrel by reducing the Teflon sleeve diameter through axial stretching. It was left in distilled water at room temperature until either tested *in vitro* or implanted in an animal.

2.2. Mechanical, morphological and permeability characterization

Uniaxial mechanical testing was performed on 4–5 mm long and 0.5–1.0 mm wide unsterilized membrane specimens in the wet state at 37 °C, using the micromechanical tester and protocol of Richardson *et al.* [27]

Scanning electron microscopy (SEM) (AMRay 1000A model Amray, Inc., Bedford, MA) provided information on the pore size, shape, and surface

characteristics of the luminal side, outside, and cross-section of the membranes. Because vacuum drying significantly distorts the material by collapsing its spongy structure, samples were frozen and then freeze-dried (Labconco Corp., Kansas City, MO) before being sputter-coated with gold–platinum (SPI sputter).

The total void volume, or porosity was calculated from the difference between the wet and the dry weights of the specimens. To measure hydraulic permeability, the volume of water passing through the wall of the tubular membrane under a fixed head of pressure, was collected for 5 min and expressed as ml min^{-1} cm^{-2} of water at 120 mmHg of hydrostatic pressure [28].

2.3. Membranes implantation procedure

Membranes, featuring a porous structure both on the inner and on the outer surface, were sterilized immediately before implantation according to the following protocol: One end of a 60 mm long membrane segment was tied off with 6–O silk ligature and the other mounted on a sterile tubing adapter attached to a sterile 10 ml syringe. A syringe pump (Harvard Apparatus, model 940, South Natick, MA) was then used to ultrafiltrate liquid through the wall of the vertically oriented membrane using 10 ml each of the following 4 solutions: (1) Sterile isotonic saline; (2) 50% ethanol; (3) 0.1 M hydrochloric acid, and (4) a final rinse of sterile isotonic saline. Sterilized membrane segments, 1.5–2.0 cm long, were implanted in the infrarenal abdominal aorta of two groups of six male Sprague-Dawley rats weighing 300–350 gm. Pentobarbital sodium anesthesia and standard microsurgical techniques using 10–0 nylon sutures (Deknatel, Inc., Division of Pfizer Hospital Product Group, Fall River, MA) were employed. Anticoagulation was not used at any time. Immediately after implantation, the prostheses were seen to undergo cycles of dilatation and recoil synchronous with the heart beat, and the same visual observation was made at time of explantation of patent prostheses.

2.4. Prostheses retrieval and histologic evaluation

After either 4 or 8 weeks the rats were deeply anesthetized with pentobarbital sodium and transcardially perfused with heparinized phosphate buffer solution (PSB) and modified Karnovsky's fixative. The grafts were then excised, opened longitudinally under magnification, and pinned in the open position for gross examination, assessment of patency, measurement of graft length and circumference, and macrophotography. The grafts were then maintained in Karnovsky's fixative until processed for histology.

Specimens for light microscopy examination were fixed in glutaraldehyde, dehydrated, embedded in paraffin, sectioned at 5 μm, and stained with hematoxylin–eosin and Gomori's trichrome. The internal capsule and wall thickness were measured at points every 50 μm along the longitudinal and transverse axis of the grafts by a computer controlled morphometric system (Bioquant IV, R & M., Biometrics, Inc., Nashville, TN). Sections for transmission electron microscopy (TEM) examination (Philips 410 model, Philips Electronic Instruments, Mahwah, NJ) were postfixed in a 1% solution of osmium tetroxide and cut at 70 nm on a Reichert ultra-microtome.

3. Results

3.1. Processing conditions

Various combinations of parameters related to the spraying and phase-inversion techniques can be used to produce white, opaque, gel-like tubular membranes with a range of diameters, wall thicknesses, porosities, and mechanical properties. The rough limits of the ranges over which these parameters can vary are summarized in Table I.

For the experiments described here, two kinds of 1.5 mm i.d. tubular membranes were fabricated: with and without a dense inner polymer layer (skin). Both types featured a porous, communicating cell wall structure and an outer porous wall. The skin was produced by first spraying the polymer solution with a single gun in the absence of a nonsolvent. After this step the deposited polymer was dried for 2 min at temperatures varying from 65° to 70 °C, using a quartz heating rod placed 4 cm below the rotating mandrel. The porous wall was subsequently formed by simultaneously spraying distilled water and the thermodynamically unstable polymer solution. Since turbidity appeared in the 1% Cardiothane $^{TH}51$ polymer solution in 2:1 THF/1,4 dioxane solvent mixture once 20 ml of distilled water had been added to 100 ml of the original solution (5:1 dilution ratio solvent/nonsolvent), we used a polymer–solvent–nonsolvent system displaying a relatively high degree of phase separation but still clear rather than turbid. This was achieved by adding 16.5 ml of distilled water to the original polymer solution, which lowered the polymer concentration in the fabricating solution to 0.86% w/v. The processing conditions used to fabricate tubular membranes with an inner skin are reported in Table II.

3.2. Physical characterization studies

Fig. 3 illustrates the results of uniaxial mechanical testing performed on samples of rat abdominal aorta

TABLE I Parameters for fabricating Cardiothane 51® tubular membranes by the spraying, phase-inversion process

1. PU solution concentration (% w/v)	0.3–2.0
2. Nonsolvent (water) in the PU solution (% v/v)	0–20
3. Gas driving pressure (KPa)	41.4–103.5
4. PU solution flow rate (ml min^{-1})	0.5–3.5
5. Nonsolvent (water) flow rate (ml min^{-1})	0.5–3.5
6. Angle between spray gun(s) and mandrel (°)	70–80
7. Distance between nozzles and mandrel (mm)	15–100
8. Mandrel diameter (prosthesis i.d.) (mm)	0.5–6.0
9. Mandrel rotation speed (r.p.m.)	100–2000
10. Carriage movement speed (cm min^{-1})	10–150
11. Internal nozzles bore (mm)	0.2–0.5

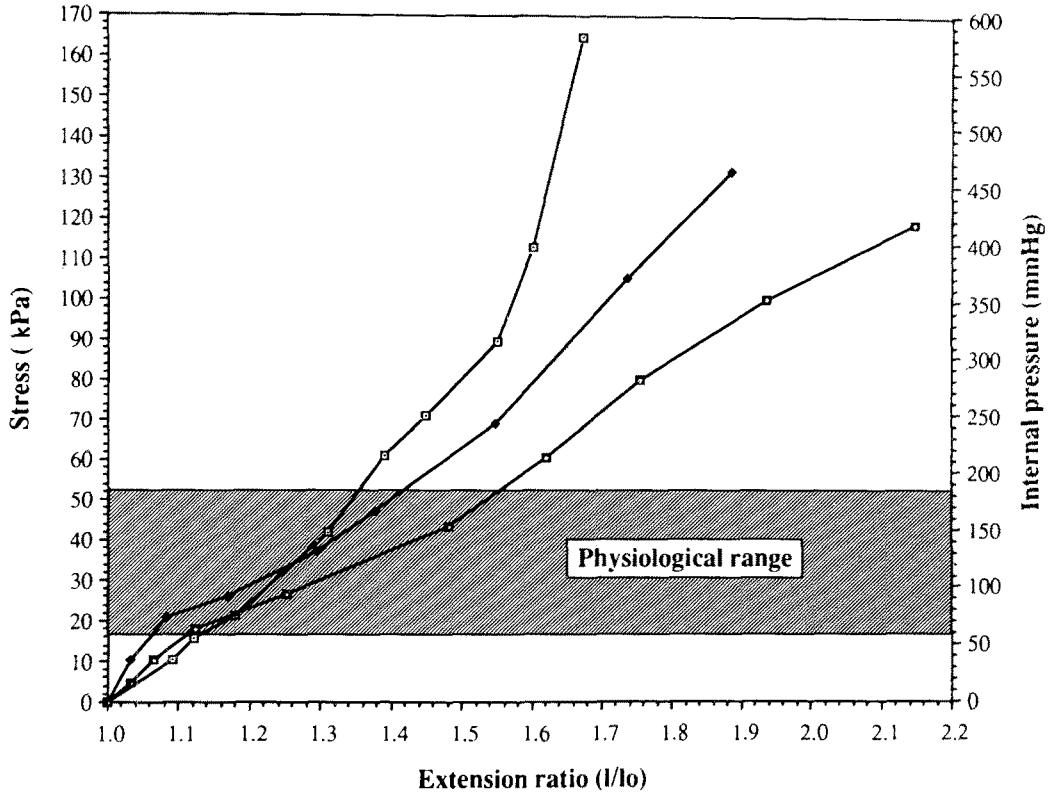

Figure 3 Stress–strain relationship: (□) Rat aorta stressed longitudinally; (◆) opened circumferential ring of membrane material; (□) longitudinal strip of membrane material. On the right axis are reported stress values expressed as mmHg of internal pressure through the relation: $\sigma = Pr/s$, where: σ = stress (wall tension); P = internal pressure; r = internal radius; s = wall thickness. The physiological range of stress encountered by the prostheses is shown by the stippled band.

or tubular membranes. Curve (a) corresponds to a freshly excised aorta stressed longitudinally; curve (b), to an opened circumferential ring of membrane material; and curve (c), to a longitudinal strip of the same material. In the physiologic range of pressure (58–184 mmHg) [29], which for these graft dimensions corresponds to a stress (wall tension) of 16.6–52.6 kPa, both longitudinal and circumferential compliance curves approximated the value for the native rat aorta tested longitudinally. An anisotropic material behaviour was observed with higher compliance under longitudinal loads than under circumferential loads at all levels of strain.

TABLE II Processing conditions to fabricate Cardiothane $^{TH}51$ tubular membranes with an inner skin and an interconnecting porous wall

Parameters	Inner skin (one gun)	Outer wall (two guns)
1. Polymer solution concentration (% w/v)	1	0.86
2. Nonsolvent (water) in the polymer solution (% v/v)	0	16.5
3. Gas driving pressure (KPa)	48.3	103.5
4. Polymer solution flow rate (ml min^{-1})	0.5	3.5
5. Nonsolvent (water) flow rate (ml min^{-1})	–	3.5
6. Angle between spray gun(s) and mandrel (°)	75	75
7. Distance between nozzles and mandrel (mm)	90	40
8. Mandrel diameter (prosthesis i.d.) (mm)	1.5	1.5
9. Mandrel rotation speed (r.p.m.)	600	600
10. Carriage movement speed (cm min^{-1})	70	70
11. Internal nozzles bore (mm)	0.3	0.3
12. Length of spray deposition (cm)	11.5	11.5
13. Volume of polymer solution used (ml)	3	50
14. Fabricating time (min)	1.5	13.5

Scanning electron micrographs of a membrane fabricated according to the methods of Tables I and II, are shown in Fig. 4. The tubular structure shows a thin (~ 10 μm) relatively smooth inner skin and a spongy porous wall approximately 350 μm thick with a porous outer surface. The wall is made of circularly oriented layers of polymeric material forming an open cell porous structure (Fig. 4a). At high magnification the outer surface shows a mesh of polymer fibres of approximately 2 μm diameter, with interfibre spaces ranging from 20–40 μm, which penetrate into the bulk of the material (Fig. 4b). A high magnification of the inner surface shows a dense structure with a few pores, ranging from 0.25–1.25 μm diameter (Fig. 4c).

The membranes exhibited a porosity of approximately 78% and the hydraulic permeability of membranes without inner skin was in the order of 4 ml min^{-1} cm^{-2} at 120 mmHg.

3.3. Macroscopic and histologic examination of the retrieved prostheses

The prostheses exhibited favourable properties for surgical handling and implantation. The material was easily penetrated with a 70 micron needle and was

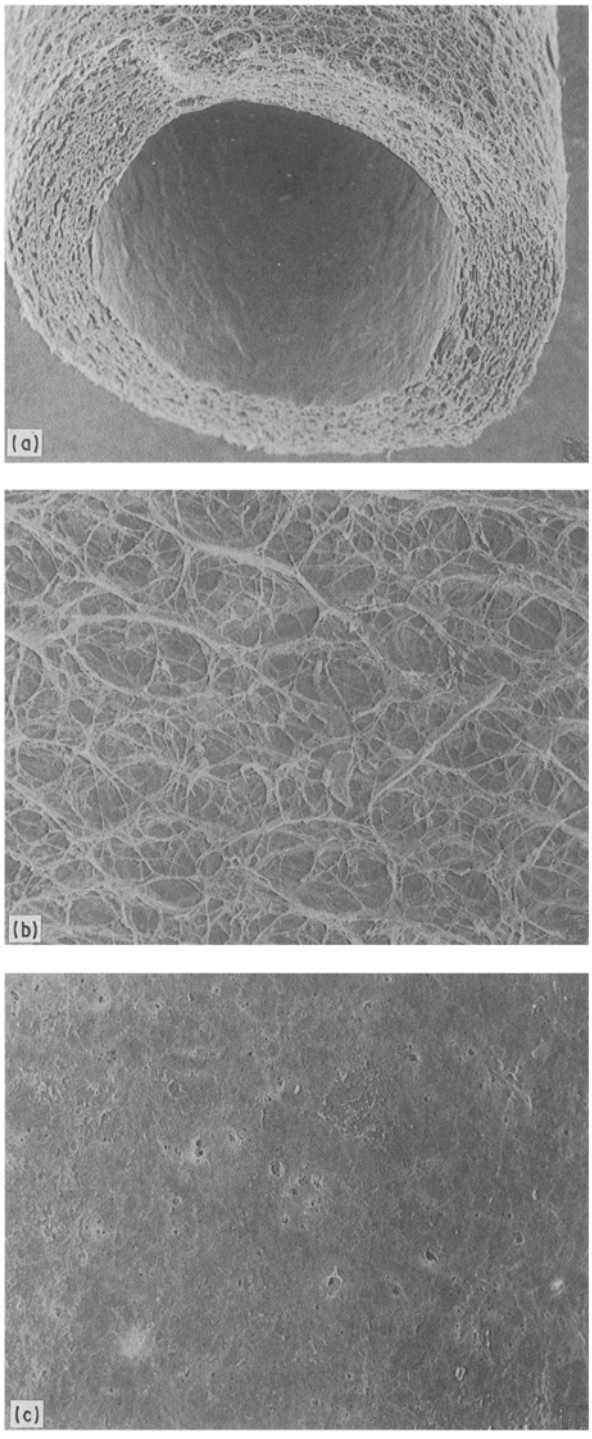

Figure 4 Scanning electron micrographs of a 1.5 mm i.d. tubular membrane with internal skin: (a) Inclined view showing the inner surface, the wall, and the outer surface (original magnification 50 ×); (b) aspect of the outer surface showing a fine mesh of polymer fibres (original magnification 200 ×); (c) aspect of the inner surface showing a dense polymer layer with sparse pores (original magnification 1600 ×).

about as tear-resistant as a human saphenous vein. The grafts were sufficiently pliant to be flexed and folded as required for suture placement, but showed adequate memory to return spontaneously to their original open, cylindrical configuration. This feature afforded visualization of the back walls of the anastomoses and facilitated needle placement. Preclotting was not employed, yet no suture hole bleeding nor leaking through the graft material was observed. Unskinned prostheses displayed a patency rate of 83% (5/6) and 50% (3/6) at 4 and 8 weeks post-implantation, respectively. At retrieval time none of these grafts showed any aneurysm formation, perigraft hematomas or rupture. All anastomoses were intact. The grafts moved freely, and external tissue reaction was minimal. Gross examination of patent grafts revealed an inner surface lined with a smooth, thin layer of transparent glistening tissue, with occasional small foci of yellow-tan staining, but no evidence of adherent thrombus or exposed polymer (Fig. 5).

Four components of the graft healing response were examined by light or electron microscopy.

1. The luminal lining: The major portion of the internal capsule of the 4 week grafts was composed of a thin tissue membrane (Fig. 6a), which at higher magnification was found to be made of a single layer of endothelial-like cells overlying several layers of myofibroblastic cells (Fig. 6b). In other regions exhibiting a less mature surface, the luminal lining was composed of isolated cells situated within a fibrin protein matrix (Fig. 6c). The internal capsule of the 8 week grafts showed a multilayered collagenous structure (Fig. 7a), almost completely lined with endothelial-like cells overlying multiple layers of myofibroblastic cells (Fig. 7b). The mean internal capsule thickness was 7.3 ± 6.9 μm for the 4 week grafts; 32.9 ± 19.6 μm for the 8 week grafts. Under TEM examination the endothelial-like cells appeared as flattened cells with elongated nuclei (Fig. 8).

2. The graft material: The polymeric material seemed to be relatively resistant to biodegradation and tissue processing and was visible as a refractile substance distributed throughout the wall of the conduit (Figs 6a–7a). Its birefringence to polarized light remained undiminished at 8 weeks compared to the appearance at 4 weeks.

3. The inflammatory reaction: In the 4 week grafts, isolated histiocytic cells were present within the graft material voids as well as adjacent to the external aspect of the prosthesis. These cells occasionally fused to form "small" giant cells. A localization of the inflammatory response to the external surface of the

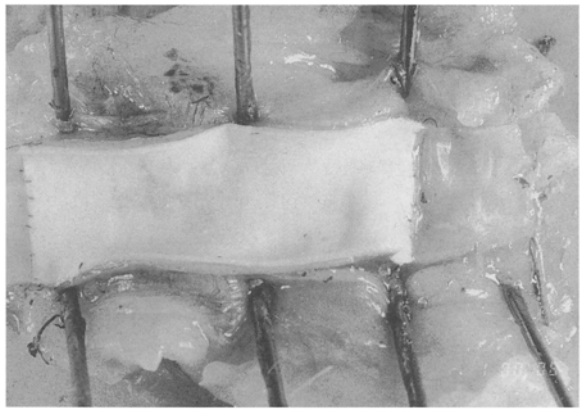

Figure 5 Prosthesis (1.5 cm long) 8 weeks after implantation. The interior is completely lined with a thin layer of transparent glistening tissue without any mural thrombus. A pale yellow stain is visible in one area of the prosthesis.

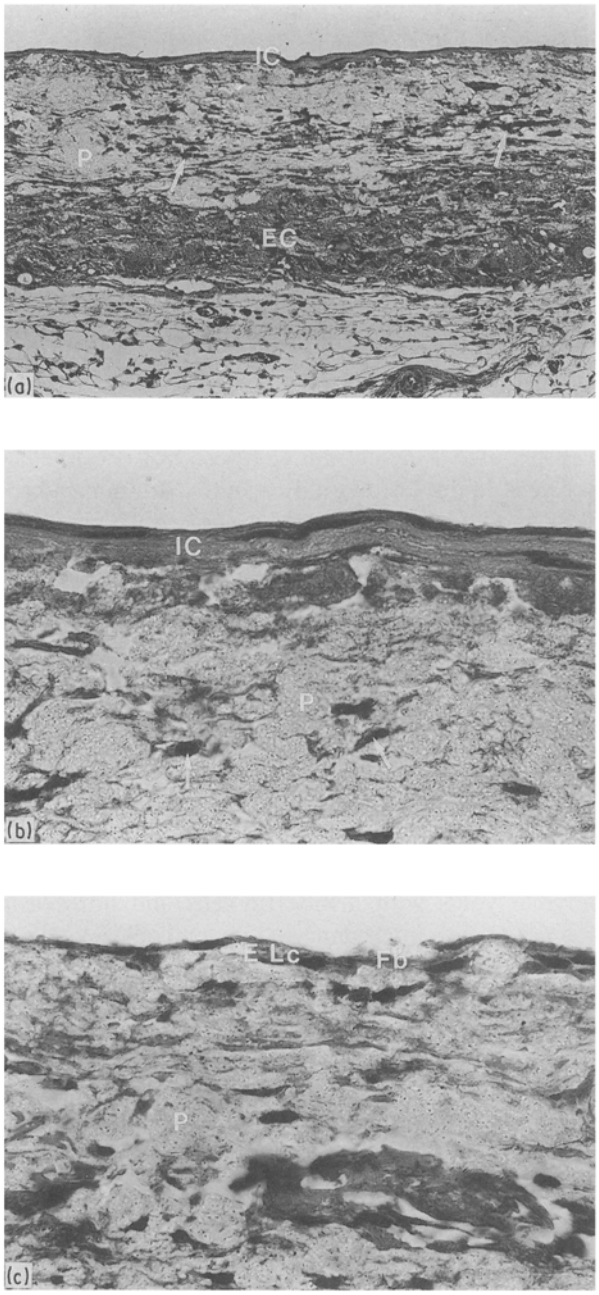

Figure 6 Light microscopy of longitudinal section of mid-portion of a graft after 4 weeks of implantation (H and E stain): (a) Three zones are recognizable: the internal capsule (IC), the graft material (P), and the external capsule (EC). Note the isolated histiocytic and fibroblastic cells (arrows) (original magnification 50 ×); (b) luminal aspect of the graft illustrating the internal capsule (IC), the graft material (P), and infiltrating histiocytic and fibroblastic cells (arrows) (original magnification 250 ×); (c) in this area the luminal aspect is composed of isolated endothelial-like cells (E-Lc) and fibrinous protein (Fb). The graft material is also recognizable (original magnification 250 ×).

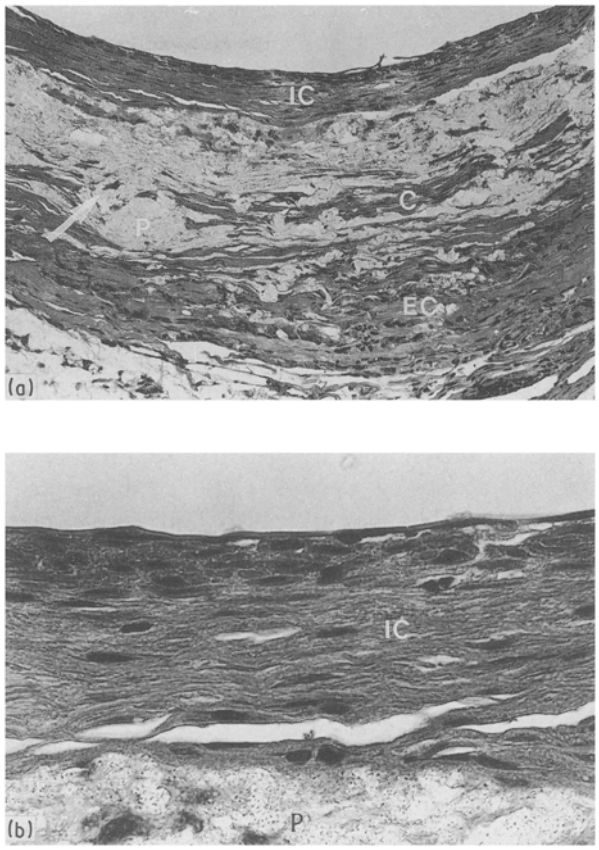

Figure 7 Light microscopy of cross-section of mid-portion of a graft after 8 weeks of implantation (H and E stain): (a) Three zones are recognizable: the internal capsule (IC), the graft material (P), and the external capsule (EC). Note the infiltrating island of collagenous tissue (C) and histiocytic inflammatory cells (arrow) (original magnification 50 ×); (b) luminal aspect of the graft illustrating the internal capsule (IC), and the graft material (P) (original magnification 250 ×).

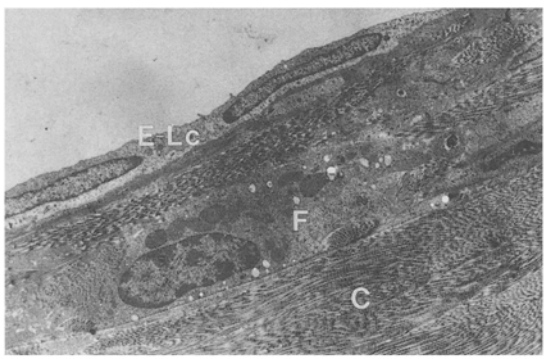

Figure 8 Transmission electron micrograph of inner capsule mid-portion of a graft after 8 weeks of implantation. The luminal aspect of the graft is composed of endothelial-like cells (E-Lc) overlying fibroblastic (F) and collagenous (C) tissue (original magnification 1000 ×).

prostheses at both time periods was also noted (Figs 6a–7a). This process of external organization formed a capsule with an indistinct line of demarcation from the region which contained the polymer. Its external aspect was clearly separated from the adjacent tissue.

4. The incorporation of native tissue: In addition to the histiocytic infiltration of the graft material voids, fibrinous protein and individual fibroblastic cells were also present in the 4 week samples, with evidence of early collagen deposition (Fig. 6a). In the 8 week samples, small islands of vascularized, organized collagenous tissue were seen in the polymer voids (Fig. 7a). The development of a mature stable luminal interface and the deposition of collagenous tissue within the grafts was well advanced by 8 weeks. Apparently, this healing process did not occur at the expense of luminal cross-sectional area, nor did it

materially affect mural thickness. The mean total wall thickness (internal capsule plus polymer region plus external capsule) was 232 ± 57 at 4 weeks, and 274 ± 128 μm at 8 weeks.

4. Discussion

Many parameters involved in a spraying technique, from polymer solution concentration to distance between nozzles and mandrel, mandrel rotation speed, and carriage movement speed, can be independently adjusted to obtain tubular membranes with different morphological and mechanical properties [22]. However, in this study, our main concern was to investigate a phase-inversion effect in a polymer solution as it is cast over a rotating mandrel. Gel-like tubular membranes were obtained through the interplay of mass transfer and phase separation which resulted from a local exchange of solvent for nonsolvent at the point where the jet streams of the spray guns converged. Porosity was proportional to the concentration of nonsolvent within the phase-inversion casting solutions [25], and we deliberately strove to obtain a highly porous structure with communicating voids.

The major advantage of this technique is its flexibility. By varying the amount of nonsolvent in the polymer solution and adjusting the mechanical parameters of the spinning process, one can vary the porosity of the tube wall over a wide range, and as a result obtain wall compliance values ranging from venous to arterial to rather rigid tube properties. The fabrication process can be adapted to a range of tubing diameters and can be adapted to conical as well as cylindrical mandrels. An asymmetric structure can be obtained if there are reasons to deposit a nonporous or minimally porous skin on the inside or outside of the tube. One could conceivably prepare the anastomotic area with properties different from those in the body of the prosthesis. Bioactive polypeptides, anticoagulants, and other growth stimulating or inhibiting factors might be incorporated into the gel-like structure by suspending or dissolving them in the solvent or in the nonsolvent (in this case, water), to achieve a slow, local release which could influence the healing process [30].

The drawbacks and uncertainties of the spraying, phase-inversion technique also need to be mentioned. We have little information regarding the shelf life and the *in vivo* durability of the Cardiothane $^{TH}51$ mesh which makes up these prostheses. The risk of aneurysm or *pseudo*aneurysm formation inherent with any weak and potentially degradable structure needs to be investigated with larger diameter grafts, where catastrophic failure is more likely to occur than in miniature grafts. Long term tissue response to the polyurethane blend, including calcification, will have to be addressed. The prostheses described here were fabricated, sterilized, and stored in the wet state, which is acceptable in an experimental laboratory, but might not be acceptable for clinical use. We need to establish whether ethanol and/or hydrochloric acid sterilization affects the integrity of the polymer mesh. Alternatively, we can pursue preliminary observations which suggest that once the curing process is completed, the prostheses can be freeze-dried, and thus become amenable to gas sterilization, without changes in the morphological or physical properties upon rewetting.

The relatively high patency rate observed in the rat abdominal aorta model is not in itself remarkable, since other authors have reported similar results [31]. This model is useful to test the mechanical properties of the graft and to study the tissue response to its gel-like structure. Mechanically the graft sustained the arterial pressure for the 8 weeks of implantation without aneurysm formation. Tissue ingrowth in the prosthetic wall was progressive and quite mature by 8 weeks. Morphologically, the newly formed vascular wall featured a neointima composed of endothelial-like cells lining an internal capsule containing fibroblast and collagen. At 4 weeks, some portions of the grafts exhibited an active endothelialization process characterized by the presence of isolated endothelial-like cells on the surface surrounded by an acellular fibrinous matrix. The grafts were almost completely endothelialized at 8 weeks. Contrary to other reports in literature [31, 32] about polyurethane grafts implanted in the rat abdominal aorta, there was no difference in the thickness of the neointima between the anastomotic area and the mid-portion of the graft. The porous graft material appeared to be intact after 8 weeks of implantation. A progressive infiltration of the polymer voids with histiocytic cells and fibroblasts was noted with interconnected microscopic islands of collagenous tissue present at 8 weeks. The deposition of collagen did not produce a rigid structure since the grafts remained compliant and pulsatile at the time of explantation.

In conclusion, the spraying, phase-inversion process allows the fabrication of gel-like, compliant tubular membranes for experimental small diameter arterial or venous substitution. Cardiothane $^{TH}51$ appears to be a suitable material for graft fabrication with adequate mechanical strength and excellent healing properties. Long term implants, both on small and large size animal models, are needed to establish the relevance of this graft fabrication technique for the clinical replacement of damaged blood vessels.

Acknowledgements

The authors wish to thank Dr Peter Richardson for the mechanical testing, Mrs Sandra Kunz for SEM, Dr Joseph Megerman for reviewing the manuscript, and the Artificial Organ Laboratory at Brown University for supporting in part, this study.

References

1. R. K. DANIEL and J. K. TERZIS, in "Reconstructive Microsurgery" (Little Brown & Co., Boston, 1978).
2. J. A. MANNICK, A. D. WHITTEMORE and N. P. COUCH, in "Vascular surgery a comprehensive review", edited by W. S. Moore (Grune & Stratton, 2nd Edn, New York, 1986).
3. C. L. VAN KAMPEN and D. F. GIBBONS, *J. Biomed. Mater. Res.* **13** (1979) 517.
4. N. JAYAKUMARY, *Biomater. Med. Dev. Artif. Organs* **12** (1985) 97.

5. W. G. PITT, K. PARK and S. L. COOPER, *J. Colloid Interface Sci.* **111** (1986) 343.
6. M. D. LELAH and S. L. COOPER, in "Polyurethane in Medicine" (CRC Press Inc., Boca Raton, FL, 1986) pp. 151–57.
7. D. J. LYMAN, J. F. FAZIO, H. VOORHEES, G. ROBINSON and D. ALBO, *J. Biomed. Mater. Res.* **12** (1978) 337.
8. K. B. SEIFERT, D. ALBO, H. KNOUWLTON and D. J. LYMAN, *Surg. Forum.* **30** (1979) 206.
9. W. M. ABBOT and R. P. CAMBRIA, in "Biologic and synthetic vascular prostheses", edited by J. C. Stanley, W. E. Burkel, S. M. Lindenauer, R. H. Bartlett and J. G. Turcotte (Grune & Stratton, New York, 1982) pp. 131–52.
10. R. E. CLARK, S. APOSTOLOU and J. L. KARDOS, *Surg. Forum.* **27** (1976) 208.
11. S. A. WESOLOWSKI, C. C. FRIES, K. E. KARLSON, M. DeBAKEY and P. N. SAWYER, *Surg.* **50** (1961) 91.
12. H. P. GREISLER, D. U. KIM, J. B. PRICE and A. B. VOORHHEES, *Surg.* **120** (1985) 315.
13. B. VAN DER LEI, Ch. R. H. WILDEVUUR, P. NIEUWENHUIS, E. H. BLAAUW, F. DIJK, C. E. HULSTAERT and I. MOLENAAR, *Cell. Tissue. Res.* **242** (1985) 569.
14. E. PELLOCK, E. J. ANDREWS, D. LENTZ and K. SEIKH, *Trans. Amer. Soc. Artif. Inter. Organs* **27** (1981) 405.
15. C. HERMANSEN, K. KRAGLUND, E. LUDWIGSEN and C. MOURITZEN, *Eur. Surg. Res.* **12** (1980) 349.
16. R. A. WHITE, *Trans. Amer. Soc. Artif. Intern. Organs* **34** (1988) 95.
17. R. A. WHITE, J. N. WEBER and E. W. WHITE, *Science* **176** (1972) 922.
18. L. F. HIRATZKA, J. A. GOEKEN, R. A. WHITE and C. B. WRIGHT, *Arch. Surg.* **114** (1979) 698.
19. D. LYMAN, D. ALBO, R. JACKSON and K. KNUTSON, *Trans. Amer. Soc. Artif. Intern. Organs* **23** (1977) 253.
20. D. ANNIS, A. BORNAT, R. O. EDWARDS, A. HIGHAM, B. LOVEDAY and J. WILSON, *ibid.* **24** (1978) 209.
21. J. LEIDNER, E. W. C. WONG, D. C. MacGREGOR and G. J. WILSON, *J. Biomed. Mater. Res.* **17** (1983) 229.
22. R. R. KOWLIGI, W. W. VON MALTZAHN and R. C. EBERHART, *J. Biomed. Mater. Res.: Appl. Biomater.* **22** (1988) 245.
23. R. S. WARD, Jr and E. NYLAS, in "Organometallic Polymers" (Academic Press, Inc., New York, 1972) pp. 219–29.
24. Biomedical Polymer Application and Fabrication Guidelines, Kontron Instruments Inc., Everett, MA (1981).
25. R. E. KESTING, in "Synthetic Polymeric Membranes. A Structural Perspective" (John Wiley & Sons, New York, 1985) 237–85.
26. H. WIJMANS, PhD thesis Twente University of Technology, Twente (1984).
27. P. RICHARDSON, A. PARHIZGAR, H. F. SASKEN, T. H. CHIU, P. AEBISCHER, L. A. TRUDELL and P. M. GALLETTI, in "Tissue Characterization by Micromechanical Testing of Growths Around Bioresorbable Implants. Progress in Artificial Organs" (1985) pp. 1015–19.
28. Vascular Graft Prostheses. ANSI/AAMI, VP20–1986, Association for the Advancement of Medical Instrumentation, Arlington, VA (1986).
29. H. J. BAKER, J. R. LINOSEY and S. H. WEISBROTH, in "The Laboratory Rat" Vol II (Academic Press, 1980).
30. G. SOLDANI, M. STEINER, M. GODDARD, G. PANOL and P. M. GALLETTI, in Abstracts of the 35th Annual Meeting of the American Society for Artificial Internal Organs, Texas, May 1989 (J. P. Lippincott Co., 1989) p. 51.
31. F. HESS, C. JERUSALEM and B. BRAUN, *J. Cardiovasc. Surg.* **24** (1983) 516.
32. *Idem., ibid.* **24** (1983) 509.

Received 7 June
and accepted 3 October